ISSN: 2634 - 8853

Journal of Engineering and Applied Sciences Technology

SCIENTIFIC Research and Community

Review Article

Open Access

Effect of Convective Surface Boundary Condition MHD Heat and Mass Transfer over a Vertical Plate with Buoyancy and Chemical Reaction

Akindele M Okedoye[1]*, Azeez A Waheed[2] and Peter O Ogunniyi[1]

[1]Department of Mathematics, Covenant University, Canaan Land, Ota, Ogun State, Nigeria

[2]Department of Mathematics, Lead City University, Ibadan, Oyo State Nigeria

ABSTRACT

The paper focuses on the heat and mass transfer over a vertical plate with buoyancy and chemical reaction under the influence of convective surface boundary conditions. We enhance and improve the work of Aziz and Makinde in order to integrate hydromagnetic mixed convection heat and mass transport over a vertical plate with a convective surface boundary condition as well as heat generation/absorption and reactivity characteristics [1,2]. Using self-similar variables, the equations governing boundary-layer flows were converted into a two-point boundary value problem, which was then solved numerically. To ensure that the asymptotic conditions is not affected for an imposed finite domain, the is taken to be large enough. The numerical computation was implemented using mathematical software Maple 2022 to execute the codes. We performed the computation in both hardware precision and arbitrary precision, by setting the digits to 20. The numerical result have been plotted to clearly show the effect of the governing parameters on the flow. In other to validate our result, we compare our results with existing published result when the improvement in the current work are taken to be zero the comparison was displayed in Table 1 which was in an excellent agreement. Our results amongst other, shows that local skin-friction coefficient, local heat and mass transfer rate at the plate surface increases with an increase in magnetic field, intensity of buoyancy force, convective heat exchange parameter and buoyancy ratio, increase in convective heat transfer increases the temperature and maximum concentration occurs with generative chemical reaction within the body of the fluid close to the surface. The effect of all other governing parameter were displayed graphically and discussed extensively.

***Corresponding author**

Akindele M Okedoye, Department of Mathematics, Covenant University, Canaan Land, Ota, Ogun State, Nigeria.
E-mail: michael.okedoye@covenantuniversity.edu.ng

Received: July 20, 2022; **Accepted:** July 23, 2022; **Published:** July 30, 2022

Keywords: Convective Surface, Buoyancy, Chemical Reaction, Heat And Mass Transfer, MHD, Boussinesq Approximations

Introduction

The study of heat and mass transfer with chemical reactions has enormous practical relevance for engineers and scientists due to its nearly universal occurrence in many scientific and technical disciplines. The current trend in chemical reaction analysis is to model the system mathematically in order to predict reactor performance. The two types of chemical reactions are heterogeneous and homogeneous, respectively. Whether they occur at an interface or as a single phase volume reaction will affect this, and the reaction rate will rely on the species concentration. The chemical and hydrometallurgical industries both involve the understanding of heat and mass transfer with chemical reactions. A crucial role is played by coupled heat and mass transfer with chemical reaction effects in the distributions of temperature and moisture over agricultural areas, the formation and dispersion of fog, orchards of fruit trees, and designs of chemical processing equipment. Omidpanah et al. attempted to approximate the unknown temperature distribution across the heater surface located on the upper wall of a two-dimensional rectangular duct in order to achieve uniform heat flow and temperature distribution over the design surface. On the other hand, improving energy efficiency is essential because energy is so scarce. Nanofluids are being employed in the heat transfer field to enhance heat transport and decrease energy waste. Liang et al. [3,4].

In their study, Mohammad et al. used well-known geometries to simulate the flow and temperature field inside hollow bricks in order to examine the transient thermal behavior in both solid and fluid zones [5]. The obtained results show that the rate of heat transmission is reduced and the wall emissivity decreases to zero in geometries with vertical rectangle sub cavities. In addition, the time needed to attain steady state is related to the total heat flux. Among the many industrial and engineering applications for which the study of flow and heat transfer due to stretching surfaces has been an important topic in the area of researchers for the past forty years are the extrusion of plastic sheets, wire drawing, paper manufacturing, polymer industries, and metal-working processes in metallurgy. Utilizing the convective surface boundary condition rather than the supposedly constant surface boundary condition seemed preferable after Aziz's research [1]. Convective surface boundary condition was used to examine a number of previous

works that had been done utilizing constant surface boundary condition. A study on MHD mixed convection flow from a vertical wall with a convective boundary condition was published by Makinde and Aziz in 2010 [6]. Makinde and Olanrewaju looked at the significant impact of thermal buoyancy on the boundary layer over a vertical wall with a convective boundary condition. The effect of thermal radiation on MHD nanofluid in a microchannel with a convective boundary condition was examined by Lopez et al. in 2017 [7,8].

There are still many aspects of the challenging problem of the mathematical description of the laminar, incompressible boundary layer flow that need to be resolved. The first semi-infinite flat plate with a continuous two-dimensional boundary layer flow was described by Blasius in 1908 [9]. At high temperatures, thermal radiation has a significant impact on the flow field, which is crucial in many engineering domains. This impact has been documented in multiple research that have explored different radiation-affected flows, including free convective laminar in a computer model for convective and radiative heat transport of very high temperature gas cooled and gaseous core reactors was released. The model's conclusions are in great agreement with correlations that have been established through experiment [10,11]. Okedoye and Ogunniyi reported MHD boundary layer flow through a moving plate with mass transfer and binary chemical reaction in [12]. Okedoye and Salawu considered and reported on unstable oscillatory MHD boundary layer flow across a moving plate with mass transfer and binary chemical reaction [13]. Okedoye and Salawu reported on the effects of nonlinear radiative heat and mass transfer on MHD flow over a stretching surface with variable conductivity and viscosity, as well as the transient effects of hydromagnetic heat and mass transfer on the flow past a porous medium with movable vertical permeable sheet [10,13]. Okedoye et al. described the flow of nanofluid via a porous medium, taking into account the characteristics of the thermophysical properties of copper (Cu) -nanofluid across a porous media in the presence of Dufour and Ohmic heating [14]. When buoyancy coefficient factor and buoyancy coefficient ratio rise, skin friction increases while the rate of heat and mass transfer at the wall decreases. Thermal radiation and porous media parameter was observed to minimize the rate of thermal boundary layer thickness of nanofluids.

Malemi et al. explored the use of passive flow control techniques, in particular vortex generators. They found that increasing injection decreased velocity while increasing suction increased it. Reduced species concentration results from an increase in the Brownian motion parameter. Okedoye et al. has received positive reviews and a number of other authors have worked in the same field [15-17].

Despite the work of multiple earlier authors, there is still a growing desire for increased energy efficiency and machine productivity. In order to integrate hydromagnetic mixed convection heat and mass transport over a vertical plate with a convective surface boundary condition as well as heat generation/absorption and reactivity characteristics, we enhance the work of Aziz and Makinde in this paper [1,2]. Using self-similar variables, the equations governing boundary-layer flows were converted into a two-point boundary value problem, which was then solved numerically. Fluid velocity, temperature, and concentration are affected visually and discussed by emerging flow controlling parameters such magnetic field, Grashof number, buoyancy factor, response parameter, heat generation/absorption, and convective heat transfer parameter. We think that our findings will complement earlier research and offer more in-depth understanding and relevant data for applications.

Problem Formulation

Consider a mixed convection flow over a vertical plate with a steady, laminar hydromagnetic linked heat and mass transfer. The fluid is taken to be Newtonian, electrically conducting, and its temperature and chemical species concentration-related changes in properties are restricted to changes in fluid density. The momentum equation accounts for the effects of buoyancy and density fluctuation (Boussinesq approximation). In addition, there is no applied electric field and all of the Hall effects and Joule heating are neglected (Figure 1). Since the magnetic Reynolds number is very small for most fluid used in industrial applications, we assume that the induced magnetic field is negligible.

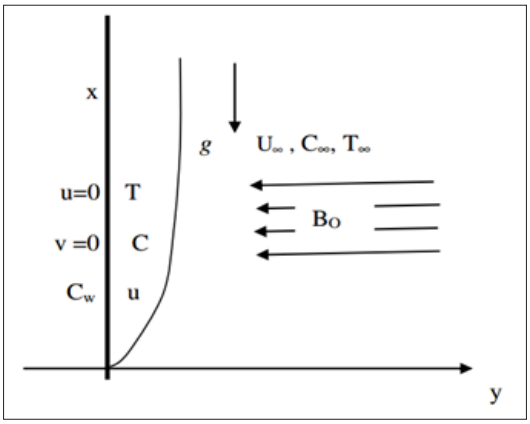

Figure 1: Flow Schematic Diagram [2]

Let the x –axis be taken along the direction of plate and y-axis normal to it. If u, v, T and C are the fluid x-component of velocity, y –component of velocity, temperature and concentration respectively, then under the Boussinesq and boundary-layer approximations, the governing equations for this problem can be written as:

$$\frac{\partial u}{\partial x}+\frac{\partial u}{\partial y}=0, \tag{1}$$

$$u\frac{\partial u}{\partial x}+v\frac{\partial u}{\partial y}=\mu\frac{\partial^2 u}{\partial y^2}-\frac{\sigma(x)B_0^2}{\rho}(u-U_\infty)+\frac{g\beta_t(x)}{\rho}(T-T_\infty)+\frac{g\beta_c(x)}{\rho}(C-C_\infty), \tag{2}$$

$$\rho c_p\left(u\frac{\partial T}{\partial x}+v\frac{\partial T}{\partial y}\right)=k\frac{\partial^2 T}{\partial y^2}+Q(T-T_\infty), \tag{3}$$

$$\rho\left(u\frac{\partial C}{\partial x}+v\frac{\partial C}{\partial y}\right)=D\frac{\partial^2 C}{\partial y^2}-G(C-C_\infty), \tag{4}$$

Where all parameters have there usual meaning.

The boundary conditions at the plate surface and far into the cold fluid may be written as

$$\left.\begin{gathered}u(x,0)=U_x, v(x,0)=0, -k\frac{\partial T}{\partial y}=h[T-T_w], C_w(x,0)=Ax^\lambda C_\infty \\ u(x,\infty)=U_\infty, T(x,\infty)=T_\infty, C(x,\infty)=C_\infty,\end{gathered}\right\} \tag{5}$$

where h is the plate heat transfer coefficient, L is the plate characteristic length, Cw is the species concentration at the plate surface, λ is the plate surface concentration exponent and k is the

thermal conductivity coefficient. The stream function, satisfies the continuity Equation (1) automatically with

$$u = \frac{\partial \psi}{\partial y} \text{ and } v = -\frac{\partial \psi}{\partial x}, \tag{6}$$

A similarity solution of Equations (1) – (6) is obtained by defining an independent variable and a dependent variable f in terms of the stream function ψ as

$$\eta = y\sqrt{\frac{U_\infty}{\nu x}}, \psi = \sqrt{\nu x U_\infty} f(\eta) \tag{7}$$

The dimensionless temperature and concentration are given as

$$\theta(\eta) = \frac{T - T_\infty}{T_w - T_\infty}, \phi(\eta) = \frac{C - C_\infty}{C_w - C_\infty}. \tag{8}$$

where T_w and C_w are the temperature and concentration of the hot fluid at the left surface of the plate. Equation (7) and (8) implies

$$\frac{\partial \eta}{\partial y} = \frac{\eta}{y}, \quad \frac{\partial \eta}{\partial x} = -\frac{\eta}{2x} \tag{9}$$

$$u = U_\infty f'(\eta), v = -\frac{1}{2}\sqrt{\nu U_\infty} x^{-\frac{1}{2}}\left(f(\eta) + \eta f'(\eta)\right) \tag{10}$$

The dimensionless velocity, temperature and concentration are given as

$$f'''(\eta) + \frac{1}{2} f(\eta) f''(\eta) - \mathrm{M}^2(f'(\eta) - 1) + \mathrm{Gr}\left(N\theta(\eta) + \phi(\eta)\right) = 0, \tag{11}$$

$$\theta''(\eta) + \frac{Pr}{2} f(\eta)\theta'(\eta) + \alpha\theta(\eta) = 0, \tag{12}$$

$$\phi''(\eta) + \frac{Sc}{2} f(\eta)\phi'(\eta) - \lambda\phi(\eta) = 0. \tag{13}$$

And the boundary conditions, after applying the similarity variables becomes

$$\left.\begin{aligned} f'(0) = 0, f(0) = 0, \frac{\partial \theta(0)}{\partial y} = -Bi\left(1 - \theta(0)\right), \phi(0) = 1 \\ f'(\eta) = 1, \theta(\eta) = 0, \phi(\eta) = 0, as\ \eta \to \infty. \end{aligned}\right\} \tag{14}$$

Where

$$\sigma(x) = \frac{\sigma_0}{x}, B = \frac{\mathrm{B}_{c,x}}{x}, \frac{D}{\rho\nu} = \frac{1}{Sc}, \frac{\mu \mathrm{Gx}}{DU_\infty} = \lambda, \frac{k}{\mu c_p} = \frac{1}{Pr}, \frac{Qx\nu}{U_\infty k} = \alpha,$$

$$\beta_0\sqrt{\frac{\sigma_0}{\rho U_\infty}} = M, \frac{g\beta_c(C_w - C_\infty)}{\rho U_\infty^2} = Gr, \frac{\beta_\tau(T_w - T_\infty)}{\beta_c(C_w - C_\infty)} = N, Bi = \frac{h}{k}. \tag{15}$$

Rate of Flow at the Wall: Engineering parameters of curiosity in the flow are skin friction coefficient c_f and Nusselt number Nu_x and local Sherwood number Sh_x defined respectively as;

$$\tau = C_f\sqrt{\frac{x}{\nu U_\infty}} = \left.\frac{df'(\eta)}{d\eta}\right|_{\eta=0}, \tag{16}$$

$$Nu = Nu_x\sqrt{\frac{U_\infty}{\nu x}} = -\left.\frac{d\theta(\eta)}{d\eta}\right|_{\eta=0},$$

$$Sh = Sh_x\sqrt{\frac{U_\infty}{\nu x}} = -\left.\frac{d\phi(\eta)}{d\eta}\right|_{\eta=0}.$$

Using similarity transformation, we have

$$\tau = \left.\frac{du}{dy}\right|_{y=0}, Nu = -\left.\frac{d\theta}{dy}\right|_{y=0}, Sh = \left.\frac{d\phi}{dy}\right|_{y=0} \tag{17}$$

Numerical Computation Technique

The solutions to the system of quasi-linear heat and mass boundary layer governing equations together with the corresponding boundary conditions was numerically solved for the infinite regime $0 < \eta < \eta_\infty$. However, for physical interpretation of results, a finite regime along direction is chosen. To ensure that the asymptotic conditions is not affected for an imposed finite domain, the is taken to be large enough. An independent grid is studied demonstrating that the numerical domain $0 < \eta < \eta_\infty$ can be divided into regular step size interval of 0.01. As such, the number of points reduced in the interval $0 < \eta < \eta_\infty$ with good accuracy. Taking $\eta_\infty = 5$, this is found to be sufficient for newton iteration convergence and the parameter range of values for the computation in this study.

To achieve the above, mathematical software Maple 2022 was used to run the code for numerical computation of the system of equations (14) – (16) along with initial and boundary conditions (17). The numerical values for the flow governing parameters are chosen as, Prandtl number values is taken as $pr = 0.71$ (plasma). The default Schmidt number value is picked as (0.62) to denote the water vapour. All emerging terms are mainly selected as follows: $Bi = 0.2$, $Gr = 0.4$, $M = 0.2$, $N = 0.5$, $\alpha = -0.3$, $\lambda = 0.8$ based on the existing related theoretical works carried out.

Maple inbuilt solver "dsolve" command with the numeric option that indicates a specific boundary value problem (BVP) was used to find a numerical solution for the self-similar ode system of BVP. In choosing a submethod for our system of equations we consider such submethods that are capable of handling harmless end-point singularities. And because of the enhancement schemes, Richardson extrapolation is generally faster and so we make use of midpoint submethod that use Richardson extrapolation enhancement or deferred correction enhancement.

We performed the computation in both hardware precision and arbitrary precision, by setting the digits to 20. In which case if digits is smaller than the hardware precision for the machine, then computations are performed in hardware precision while if digits is larger, then computations are performed in Maple floating point. In both cases, many of the more computationally intensive steps are performed in compiled external libraries. (Ascher, Mattheij and Russell, 1995 and Ascher and Petzold, 1998). Having satisfying the above, the return value of dsolve and the manipulation of the input system is controlled by the following three optional equations, which are discussed in dsolve[numeric]. We employed the odeplot function to plot solution curves obtained from the output of a call to dsolve/numeric capitalizing on the flexibility in the specification of the coordinates. The result of a call to odeplot is rendered by the plotting device. The graphical result are then displayed by invoking display command.

Results and Discussion

The governing equations (9) - (11) subject to the boundary conditions (12) - (13) are integrated as described in Section 3. Numerical results are reported in the Tables 1 - 2 and Figures 2 -

10. The Prandtl number was taken to be $Pr = 0.72$ which corresponds to air, the values of Schmidt number (Sc) were chosen to be $Sc = 0.2, 0.62, 0.78, 2.62$, representing diffusing chemical species of most common interest in air like H_2, H_20, NH_3 and Propyl Benzene respectively. Attention is focused on positive values of the buoyancy parameters that is, Grashof number $Gr>0$ which indicates that the chemical species concentration in the free stream region is less than the concentration at the boundary surface) and buoyancy ratio $N < 1$ implies mass buoyancy dominate while $N >1$ indicates thermal buoyancy dominate. Also, $\lambda<0$ and $\lambda>0$ represent generative and destructive chemical reactions, respectively. While $\alpha < 0$ and $\alpha > 0$ indicate heat generation and heat absorption, respectively.

Validity of Result

A comparison with previously published work is performed and excellent agreement between the results is obtained. The results are presented graphically and the conclusion is drawn that the flow field and other quantities of physical interest are significantly influenced by these parameters. In order to benchmark our numerical results, we have compared the plate surface temperature $\theta(0)$ and the local heat transfer rate at the plate surface $\theta'(0)$ in the absence of magnetic field, mass buoyancy, buoyancy forces ratio, heat generation/absorption and generative/destructive chemical reaction for various values of with those of Aziz (2009) and Makinde (2010) found them in excellent agreement as displayed in Table 1.

Table 1: Comparison with Existing Results for $M= Gr = \lambda = \alpha =0.0$, $Pr =0.72$, $Sc =0.63$ and for Various Convective Surface Boundary Condition (Bi)

Bi	Aziz [1]		Makinde [2]		Present Result	
	$\theta(0)$	$\theta'(0)$	$\theta(0)$	$\theta'(0)$	$\theta(0)$	$\theta'(0)$
0.05	1447	0.0428	0.14466	0.04276	0.144565	0.042772
0.10	0.2528	0.0747	0.25275	0.07472	0.252612	0.074739
0.20	0.4035	0.1193	0.40352	0.11929	0.403336	0.119333
0.40	0.5750	0.1700	0.57501	0.16999	0.574767	0.170093
0.60	0.6699	0.1981	0.66991	0.19805	0.669697	0.198182
0.80	0.7302	0.2159	0.73016	0.21586	0.729978	0.216018
1.00	0.7718	0.2282	0.77182	0.22817	0.771652	0.228348
5.00	0.9441	0.2791	0.94417	0.27913	0.944125	0.279375
10.00	0.9713	0.2871	0.97128	0.28714	0.971260	0.287402
20.00	0.9854	0.2913	0.98543	0.29132	0.985420	0.291592

Rate of Heat and Mass Transfer at the Wall

In Table 2, we displayed the local skin friction together with the local heat and mass transfer rate at the plate surface and the effect of various governing parameter on the flow rate at the wall was discussed. From the the table, it was found that the local skin-friction coefficient, local heat and mass transfer rate at the plate surface increases with an increase in magnetic field (M), intensity of buoyancy force (Gr), convective heat exchange parameter (Bi) and buoyancy ratio (N). The consistency is established by the fact that Hartmann number which arises as a result of Lorentz force lowers the velocity of the fluid. This in turn result in higher skin friction as deduced from this study. However, with reduced velocity, the effect of heat generated as a result of internal friction is also reduced as we can see, it will result into decrease in temperature due to energy leak through the surface. This same phenomenum applies to reactant concentration hence rate of mass transfer at the wall increases. The reson for increase skin friction, Nusselt and Sherwood number is obvios. The local skin friction and heat transfer rate increases for increase in generative chemical reaction and decreases for destructive chemical reaction while the mass transfer rate at the wall increases in both scenarios. We also observed that, an increase in heat generation deceases the skin friction coefficient and, heat and mass transfer rate at the wall, while increase in heat absorption brings about increase in skin friction mass transfer rate at the wall while heat transfer rate at the wall decreases with an increase in heat absorption. Skin friction is observed to decrease with increase in Prandtl number while heat transfer rate increases with increases with increase in Prandtl number. Increase in Schmidt number (Sc) causes a decrease in both skin friction and surface heat transfer rate and an increase in the surface mass transfer rate.

Velocity distribution

In Figure 2 we demonstrates how increasing magnetic parameters result in higher velocity profiles. With increase in Hartmann number, Lorentz force which is an opposition to flow velocity is set up, which is generally know to retard the velocity but, in this case the effect of this force is only significant far away fro the the plate down the stream. The boundary layer thickness was also observed to decline an increase Hartmann number (M). in Particular, 0.6 unit of velocity would be maintained at distance 1.24, 0.43, 0.29 and 0.08 unit from the plate for values of Hartmann number 0.0, 2.0, 4.0 and 10 respectively. This is useful when a fix values of velocity is required for any value of Lorentz force. It is important to note that the velocity starts from a zero value at the plate surface and increases to the stipulated free stream value far away from the plate surface satisfying the free stream boundary condition for all parameter values. Thus increase in this opposing force will definitely retard the velocity and hence. Figure 3 shows how the velocity profiles change as the reactivity parameter increases. From the figure, it could be seen that velocity increases with an increase in generative chemical reaction. More importantly, increasing the generative reaction parameter from 0.4 to 0.6 (50% increase) brings about velocity increase from 1.16 to 1.39 (39% increase) at 1.8 unit away from the plate with surge in velocity ( ) occurring for generative chemical reaction while for destructive chemical reaction, increasing the reaction parameter from 0.8 to

4.8 (500% increase) reduces the velocity from 0.82 to 0.71 (13% decrease) at 1.8 unit away from the plate. In Figure 4 shows the relationship between buoyance ratio and velocity distribution. We observed from the figure that as mass buoyancy reduces velocity increases. Thus it coud be affirm that mass buoyancy aids the development of flow velocity. The reverse is the case for thermal buoyancy which. It should be pointed out that, indicate mass buoyance dominate while imply thermal buoyancy dominates. This is seen clearly in Figure 5, as the buoyance parameter (mass) increases the velocity also rises. Thus the velocity grows as the ratio of thermal buoyancy to mass buoyancy shrinks. From Figure 6 we observed that increase in heat generation increases velocity while increase in heat absorption brings about decline in velocity. Thus it could be deduced that heat generation aids velocity while heat absorbtion decreases velocity and heance, when velocity is to minimized in this situation, the heat in the system could be absorbed from the system, that is heat generation/absorbtion could be used to control velocity in MHD flow convective boundary condition.

Table 2: Effect of Flow Governing Parameters on Flow Rate at the Wall

M	Bi	λ	N	Gr	α	Pr	Sc	$f''(0)$	$\phi'(0)$	$\theta'(0)$
0.0								0.71208989	0.92024478	0.15078724
2.0								2.17338186	0.94338968	0.15318298
4.0								4.10068198	0.95612418	0.15423928
10.0								10.04479415	0.96956714	0.15520860
	0.1							0.72636653	0.92059158	0.08598420
	1.0							0.81327394	0.92292218	0.38197620
	2.0							0.83923013	0.92359768	0.47293428
	8.0							0.86827576	0.92431363	0.57617066
		-0.6						1.44438116	1.11291122	0.15376577
		-0.4						1.14444832	0.32153740	0.15262579
		0.8						0.74577670	0.92114689	0.15089099
		4.8						0.60021742	2.19492914	0.15029419
			0.1					0.70952623	0.92014185	0.15077375
			0.6					0.75473534	0.92138411	0.15091964
			1.5					0.83371199	0.92345440	0.15116701
			2.5					0.91829862	0.92559780	0.15142255
				0.0				0.38660402	0.91190311	0.14974523
				0.4				0.74577670	0.92114689	0.15089099
				0.8				1.07466952	0.92902770	0.15179973
				1.4				1.53173947	0.93930136	0.15290277
					-0.6			0.73207013	0.92069777	0.16050997
					-0.3			0.75364342	0.92138607	0.14563700
					0.3			0.29473238	0.90551064	0.36062843
					0.6			0.63230662	0.91718436	0.20000936
						0.001		0.75651757	0.92149187	0.14689555
						0.710		0.74577670	0.92114689	0.15089099
						4.000		0.72721917	0.92053961	0.16028127
						7.000		0.72135823	0.92033077	0.16431541
							0.2	0.75871718	0.90336974	0.15095869
							0.62	0.74577670	0.92114689	0.15089099
							2.00	0.71550882	0.97328272	0.15073827
							6.00	0.67175659	1.08647200	0.15053437

Energy distribution

In figure 7, increase in heat generation increases the bulk temperature of the system while increase in heat arbsorbtion brings about decrease in the temperature of the system. In particular, at the plate, increasing heat generation from 0.3 to 0.6 (50% increase) results in temperature increase from -0.61 to -0.42 (31% increase), and increase heat absrobtion from by 50% increases the temperature by 120%. The effect the ratio of momentum diffusivity to thermal diffusivity on temperature is displayed in Figure 8 for heat generation (α = -3) and heat absorbtion (α = 3). It should be noted that, when Pr<1 thermal diffusivity dominate and when Pr > 1 momentum diffusivity dominates. Thus from this figure, it could be seen that decrease in thermal diffusivity increases the temperature while increase in momentum diffusivity decline the temperature. When α = -3, the temperature profiles are reduced as the Prandtl number values rise. Additionally, the temperature increases when Prandl number increases for Pr <1 and decreases when Prandtl number values increases for Pr >1 until about 2.5 unit away from the plate when the scebario is reversed. The effect of Hartmann number on temperature distribution id displayed in Figure 9. Increase in Hartmann number result in increase temperature. This is due to increase in internal friction as a result of Lorentz force which opposes the velocity of the fluid. More importantly, temperature at the plate increases by from 0.65 to 1.09 (67.7%), 1.09 to 1.4 (28.4%), and 1.4 to 1.8 (28.6%) when Hartmann number (M) increases from 0 to 2.0, 2.0 to 4.0 (50%) and 4.0 to 10.0 (150%) respectively. Figure 10 shows the effect convective heat transfer parameter (Bi) on

temperature distribution. From the figure, increase in increases the temperature. It could also be seen from the figure that the effect of convective heat transfer parameter becomes less significant as it becomes large in particular, at the plate, θ (0)~0.15,0.61,0.8 and for *Bi* = 0.1, 1.0, 2.0, and 8.0 respectively It is worth mentioning that the species concentration is highest at the surface and decline to zero far away from the plate thereby satisfying the prescribed boundary conditions.

Concentration Distribution

The impact of various Schmidt numbers on Species concentration is shown in Figure 11. We observed that as viscousity of the reactant increases, the concentration boundary layer increases similarly, increases in mass diffusivity increases the species concentration and hence the boundary layer also increases. This effect is more pronounced withing the body of the fluid away from the plate and before the free stream. We displayed th effect of reactivity parameter on reactant centration in Figure 12. The figure shows that increase in generative chemical reaction parameter brings about increase in reactant concentration while destructive chemical reaction result in decrease in reactant concentration. It is note worthy to mention that maximum concentration occurs with generative chemical reaction withing the body of the fluid close to the surafe. This in indicated by the presence of concave lines representing generative chemical reaction situation.

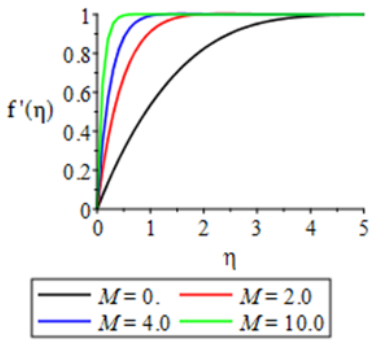

Figure 2: Efect of Magnetic Parameter on Velocity Parameter on Velocity

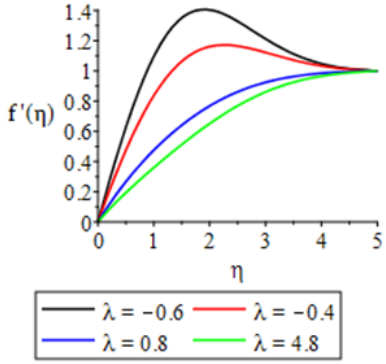

Figure 3: Efect of Reactivity Parameter on Velocity

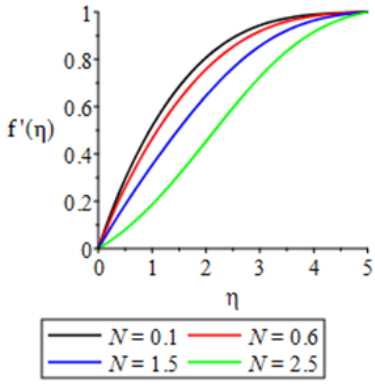

Figure 4: Efect of Buoyancy Ratio on Velocity

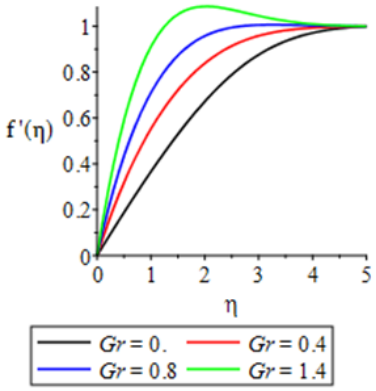

Figure 5: Efect of Buoyancy Parameter on Velocity

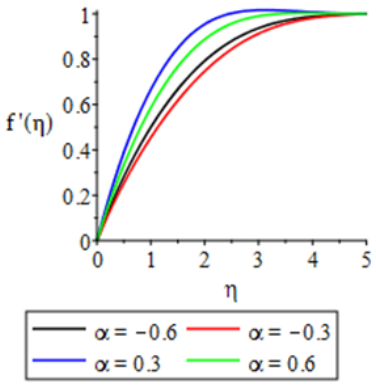

Figure 6: Efect of heat Source/Sink on Velocity

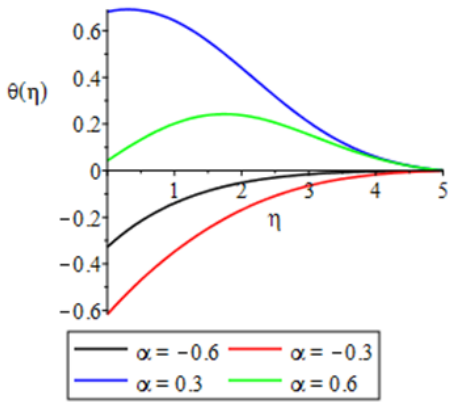

Figure 7: Efect of Heat Source/Sink on Temperature

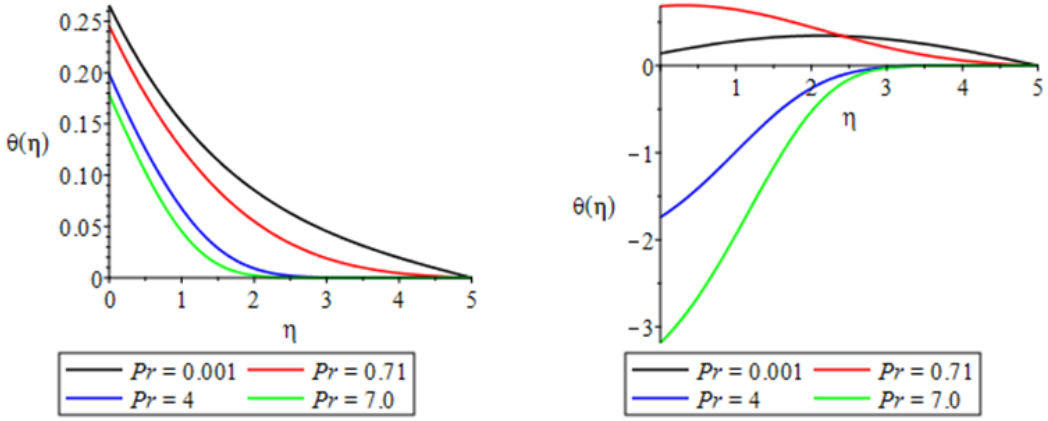

Figure 8: Efect of Prandtl number on temperature, (a) α = -3, (b) α = 3

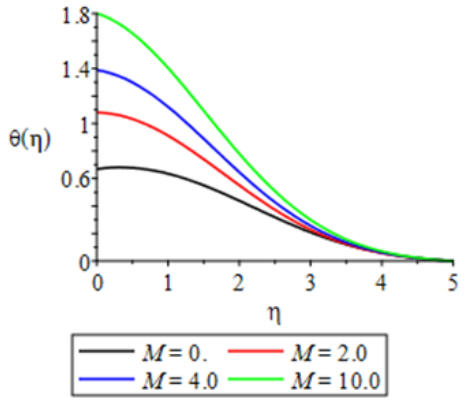

Figure 9: Efect of Hartman number on temperature during heat absorpion

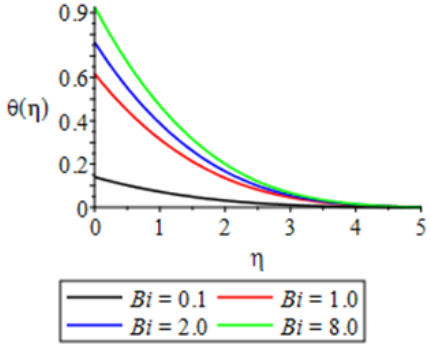

Figure 10: Efect of Convective heat transfer on temperature during heat absorpion

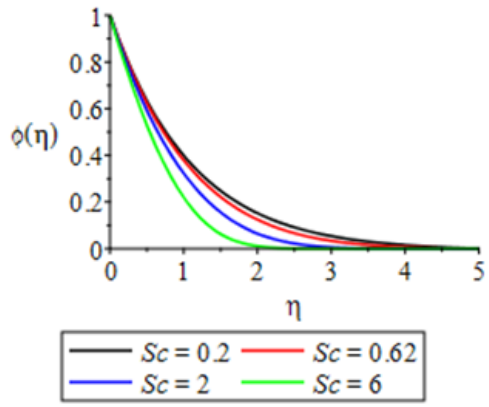

Figure 11: Efect of Shmidt Number on Concentration Distribution.

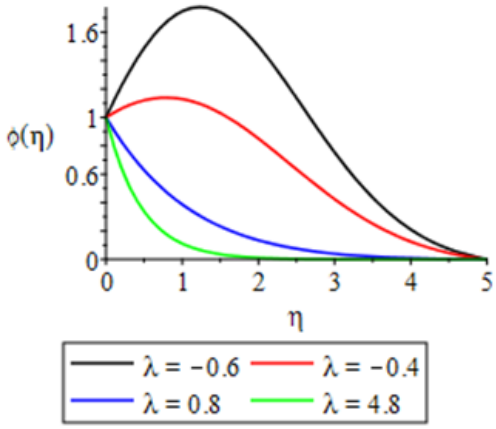

Figure 12: Efect of Reactivity Parameter on Temperature Distribution.

Conclusions

This study present Effect of convective surface boundary condition MHD heat and mass transfer over a vertical plate with Buoyancy and generative/destructive Chemical Reaction in the presence of magnetic field subject to convective heat transfer between the system and the immeadiate surrounding. The effect of applied electric field, the induced magnetic field and all of the Hall effects and Joule heating are neglected. The mathematical equations describing the flow problem are obtained using Boussinesq approximation and

are converted to ordinary differential equations using appropriate similarity transformation variables. The solutions to the system of quasi-linear boundary layer governing equations together with the corresponding boundary conditions was numerically solved for the infinite regime . To ensure that the asymptotic conditions is not affected for an imposed finite domain, the is taken to be large enough. The numerical computation was implemented using mathematical software Maple 2022 to execute the codes. We performed the computation in both hardware precision and arbitrary precision, by setting the digits to 20. The numerical result have been plotted to clearly shows the effect of the governing parameters on the flow. In other to validate our result, we compare our results with existing result when the improvement in the current work are taken to be zero. The comparsion was displayed in Table 1 where an excellent agreement with previously published work was obtained. From the present work, the following deduction could be drawn:

- local skin-friction coefficient, local heat and mass transfer rate at the plate surface increases with an increase in magnetic field (M), intensity of buoyancy force (Gr), convective heat exchange parameter (Bi) and buoyancy ratio (N).
- local skin friction and heat transfer rate increases for increase in generative chemical reaction and decreases for destructive chemical reaction
- an increase in heat generation deceases the skin friction coefficient and, heat and mass transfer rate at the wall,
- increase in heat absorption brings about increase in skin friction and mass transfer rate at the wall
- increase in Prandtl number result in increase in Skin friction and Nusselt number
- Increase in Schmidt number (Sc) causes a decrease in both skin friction and surface heat transfer rate.
- boundary layer thickness was also observed to decline an increase Hartmann number (M).
- velocity increases with an increase in generative chemical reaction.
- decrease in mass buoyancy increases velocity distribution.
- velocity grows as the ratio of thermal buoyancy to mass buoyancy shrinks.
- increase in heat generation increases velocity while increase in heat absorption brings about decline in velocity.
- increase in heat generation increases the bulk temperature of the system while increase in heat arbsorbtion brings about decrease in the temperature of the system.
- when thermal diffusivity dominate and when momentum diffusivity dominates.
- Increase in Hartmann number result in increase temperature.
- increase in convective heat transfer increases the temperature.
- maximum concentration occurs with generative chemical reaction within the body of the fluid close to the surface.

Nomenclature

x, y	flow axis	Greek Symbol	
u, **v**	Velocity component along x and y-axis	ρ	fluid density
T	Non-dimensional Temperature field	**σ**	Electrical conductivity
C	Non-dimensional Species concentration field	**ψ**	stream function
g	Acceleration due to gravity	**Dimensionless group**	
B_0	Magnetic field of uniform strength	***Bi***	Convective heat transfer
T_w	surface temperature	θ	dimensionless temperature
T_∞	ambient temperature	ϕ	dimensionless concentration
C_w	surface concentration	*Gr*	Grashof number for mass transfer
C_∞	ambient concentration	N	buoyancy ratio
B_t	Volumetric coefficient of thermal expansion	λ	Chemical reaction parameter
B_C	Volumetric coefficient of mass expansion	α	heat generation parameter
k	thermal conductivity	M	Magnetic parameter
c_p	specific heat capacity at constant pressure	***Pr***	Prandtl number
D	Molecular diffusivity	***Sc***	Schmidt number
U_∞	ambient velocity	***Nu***	Nusselt number
Q	Heat source/sink parameter	***Sh***	Sherwood number
G	reactivity parameter	**Subscript**	
		∞	ambient condition
		w	wall condition

Authour Contribution
All authours contributed equally

Conflict of Interest: The authours declare that there are no conflict of interest.

Acknowledgements: The authors would like to appreciate and thank Covenant University management for providing the enabling environment, research facilities. Also, we thank the anonymous referees for their useful suggestions that leads to improvement of the result.

References

1. Aziz A (2009) A similarity solution for laminar thermal boundary layer over a flat plate with a convective surface boundary condition, Communication Nonlinear Science Numerical Simulation 14: 1064-1068.
2. Makinde OD (2010) Similarity solution of hydromagnetic heat and mass transfer over a vertical plate with a convective surface boundary condition. International Journal of the Physical Sciences 5: 700-710.
3. Omidpanah M, Gandjalikhan Nassab SA (2019) Inverse Boundary Design Problem of Combined Radiation Convection Heat Transfer in a Duct with Diffuse-Spectral Design Surface. Thermal Science 23: 319-330.
4. Liang G, Mudawar I (2019) Review of single-phase and two-phase nanofluid heat transfer inmacro-channels and micro-channels. International Journal of Heat and Mass Transfer 136: 324-354.
5. Mohammad Omidpanaha, Seyed Ali Agha Mirjalily, Hadi Kargarsharifabad, Shahin shoeibi (2021) Numerical Simulation of Combined Transient NaturalConvection and Volumetric Radiation inside Hollow Bricks. Journal of Heat and Mass Transfer Research 8: 151-162.
6. Makinde OD, Aziz A (2010) MHD mixed convection from a vertical plate embedded in a porous medium with a convective boundary condition. Int J Therm Sci 49: 1813-1820.
7. Makinde OD, Olanrewaju PO (2010) Buoyancy efects on thermal boundary layer over a vertical plate with a convective surface boundary condition. J Fluids Eng 132: 44502
8. Lopez A, Ibanez G, Pantoja J, Moreira J, Lastres O (2017) Entropy generation analysis of MHD nanofuid fow in a porous vertical microchannel with nonlinear thermal radiation, slip fow and convective–radiative boundary conditions. Int J Heat Mass Transf 107: 982-994
9. Blasius H (1908) Grenzschichten in flüssigkeiten mit kleiner reibung. Z Angew Math Phys 56: 1-37.
10. Okedoye AM, Salawu SO (2020) Transient heat and mass transfer of hydromagnetic effects on the flow past a porous medium with movable vertical permeable sheet. Int J of Applied Mechanics and Engineering 25: 175-190.
11. Anghaie S, Chen G (1998) Application of computational fluid dynamics for thermal analysis of high temperature gas cooled and gaseous core reactors. Nucl Sci Eng 130: 361-373.
12. Okedoye AM, Ogunniyi PO (2019) MHD Boundary Layer Flow Past a Moving Plate with Mass Transfer and Binary Chemical Reaction. Journal of the Nigerian Mathematical Society 38: 89-121.
13. Okedoye AM, Salawu SO (2019) Unsteady oscillatory MHD boundary layer flow past a moving plate with mass transfer and binary chemical reaction. SN Applied Sciences 1: 1586
14. Okedoye AM, Damisa JS, Malemi BB, Kelvin O Ogboru (2022) Buoyancy Effect on MHD Nanofluid flow over a Porous Medium In the presence of Dufour and Ohmic Heating. IOSR Journal of Mathematics (IOSR-JM) 18: 26-39.
15. Beauty B Malemi, Kelvin O Ogboru, Akindele M Okedoye (2022) Heat and Mass Transfer Effects on Passive Control MHD Flow of Nanoparticles with Variable Thermophysical Properties. IRE 1703326 ICONIC Research and Engineering Journals 5: 13-28
16. Akindele M Okedoye, Kelvin O Ogboru, John Damisa, Beauty B Malemi (2022) Two-Dimensional Dissipative Non-Slip MHD Flow of Arrhenius Chemical Reaction with Variable Properties. International Journal of Advances in Engineering and Management (IJAEM) 4: 357-371.
17. Akindele M Okedoye, Sulyman O Salawu (2019) Effect of Nonlinear Radiative Heat and Mass Transfer on MHD Flow over a Stretching Surface with Variable Conductivity and Viscosity. Journal of the Serbian Society for Computational Mechanics 13: 86-103.